 MCB, vol.2, no.2, pp.53-61, 2005

Remodeling of Strain Energy Function of Common Bile Duct post Obstruction

Quang Dang[1], Hans Gregersen[2], Birgitte Duch[2] and Ghassan S. Kassab[1]

Abstract: Biliary duct obstruction is an important clinical condition that affects millions of people worldwide. We have previously shown that the common bile duct (CBD) undergoes significant growth and remodelling post obstruction. The mechanical stress-strain relation is expected to change due to growth and remodeling in response to obstruction and hence pressure-overload. The objective of the present study was to characterize the material properties of the CBD of the sham group and at 3 hours, 12 hours, 2 days, 8 days and 32 days (n=5 in each group) after obstruction. The Fung's exponential strain energy function was used to relate stress to strain of the normal and remodeled ducts. The Marquardt-Levenberg and genetic algorithm methods were used for the determination of material constants for the exponential strain energy function. The elastic constants obtained by the two methods did not differ ($p>0.254$). We obtained stable and convergent material constants at every time point. The material constant that dictates the nonlinear rate of change in the circumferential stress with respect to strain increased significantly after obstruction acutely in the first 12 hrs., decreased at 2 days and finally increased montonically during the remaining 30 days. The acute initial increase in stiffness was simply due to the elastic response. The chronic remodeling process results in an initial circumferential softening followed by stiffening of the CBD. This study has important clinical significance for patients with CBD obstruction and for endoscopists and surgeons who treat the condition.

keyword: Biomechanics, Zero-Stress State, Pressure-Overload, Marquardt-Levenberg, Genetic Algorithm

1 Introduction

The biliary duct system serves to transport bile acids and fluid from either the liver or gall bladder to the duodenum by passing it through the sphincter of Oddi. The common bile duct (CBD) has been described as a passive conduit consisting mainly of connective tissue with a high collagen content and only few smooth muscle cells (Hauke and Mark, 1965; Frierson, 1989). Obstruction of the CBD leads to an accumulation of bile and hence an increase in the pressure of the hepatic ducts. Biliary duct obstruction is an important clinical condition that stems from cholelithiasis, neoplasm in the wall or most commonly gallstones. Gallstone disease is a world-wide health problem affecting more than 20 million people in the United States alone (Roslyn and DenBesten, 1990). Biliary obstruction is a painful condition that affects liver function and the enterohepatic circulation of bile acids. Obstruction of this circulation results in malabsorption.

The pressure-overload secondary to obstruction causes an increase in circumferential, longitudinal and radial stresses and strains in the CBD. The increased mechanical stresses and strains serve as stimuli for growth and remodeling of soft tissue (Fung, 1993) which can alter the mechanical properties of the tissue. The mechanical properties of a tissue can be quantitatively described by a constitutive equation in the form of a stress-strain relation. In the theory of elasticity, it is well known that a constitutive relation can be formulated in terms of a strain energy function which represents the strain energy per unit mass or volume of the material. The stress is related to the strain by differentiation of the strain energy function (Green and Adkins, 1960). There are numerous mathematical forms for the strain energy function in the literature (Abe, Hayashi, and Sato, 1996; Fung, 1993). For example, Patel and Vaishnav (1973) proposed the polynomial form while Hayashi and colleagues prefer the logarithmic form by (Hayashi, 1993). The most widely used strain energy function, however, is Fung's exponential form mainly because it is the only orthotropic form that can be inverted; i.e., to derive analytically the tensorial strain-stress relationship from the stress-strain relationship (Fung, 1979). Regardless of the form, the strain energy function is a phenomenological mathematical ex-

[1] Department of Biomedical Engineering, University of California, Irvine.

[2] Center for Sensory-Motor Interaction, Aalborg University and Center of Excellence for Visceral Biomechanics and Pain, Aalborg Hospital, Aalborg, Denmark.

pression that relates the strain to the strain energy through a number of material parameters. The empirical parameters can be determined by "fitting" the mathematical expression to the experimental data of stress-strain relation. In this way, the material properties can be described in terms of a set of material parameters or constants for the tissue of interest.

The present study has several objectives. First, we wish to express the stress-strain relation of the CBD in terms of an exponential strain energy function. Second, we will apply the conventional Marquardt-Levenberg method and the more recent genetic algorithm method to determine the coefficients of the exponential strain energy function. Third, we will examine the changes in the material constants to describe the remodeling of the material properties of the CBD before and after occlusion. In the process, we shall quantify the remodeling of the CBD and understand the changes in the material properties of the tissue. Such information is important in clinical decision-making with respect to when and how to intervene. The physiological implications and the potential applications of the results will be discussed.

2 Methods

2.1 Available Data

Duch et al (2002) have recently described the methods of preparation, measurements and morphometric and mechanical analysis of normal and obstructed porcine CBD. Briefly, thirty female pigs were divided into five groups (n=5 in each group). Five of the pigs in each group were then subjected to CBD obstruction for 3 hours, 12 hours, 2 days, 8 days or 32 days, respectively, while the sixth pig was sham operated. The CBD was ligated (complete obstruction) approximately 1 mm from the duodenal wall. The pressure in the CBD was measured with a needle inside the duct before and after ligation.

At a scheduled time, the pigs were anesthetized again and body weight and bilirubin were measured. The CBD was harvested for *ex vivo* mechanical distension and the animal was sacrificed. The CBD was immediately transferred to an organ bath containing 22˚C oxygenated (95% O_2 and 5% CO_2) calcium-free Krebs-Ringer solution with 95 mg/l EGTA (to abolish muscle contractions) and 60 g/l Dextran (to maintain colloid osmotic pressure) at pH=7.4. The studies were done at room temperature since previous studies have shown that the mechanical properties of soft tissues do not strongly depend on temperature (Hasberry and Pearcy, 1986). The proximal end of the segment was tied over a tube connected to an infusion system and the other end was ligated as close to the sphincter of Oddi as possible. A roller pump was used for the infusion or withdrawal of Krebs-Ringer solution into the duct (Ole Dick, Instrumentmakers Aps, Denmark). The infusion or withdrawal rates were identical at 3.33 kPa/min. The volume rate was set at 0.5-8.0 ml/min, depending on the size of the CBD. When the pressure reached 5 kPa, the flow was reversed for the same time period as the infusion to ensure that the withdrawn volume equaled the infused volume. Six cycles were sufficient to obtain reproducible results (Gregersen and Kassab, 1996). After preconditioning, the passive distension experiment was executed. A Sony CCD camera and a VCR provided simultaneous recordings of outer dimension (diameter and length) of the CBD at the various imposed pressures.

After the distension protocol, the CBD segment was removed from the organ bath and a ring (2 mm wide) was cut from each of four locations along the length of the segment for zero-stress measurements (Gregersen, Kassab, and Fung, 2000). The ring was kept in oxygenated Krebs-Ringer solution in a well and visualized under a microscope (Zeiss, Stemi 2000-C) with a video camera (Sony CCD). The ring in the no-load state was cut radially which relieved the residual strain and opened into a sector. A photograph of the sector at the zero-stress state was obtained 20 minutes after the radial cut was made. The image was used for measurement of circumferences for calculation of strain as described below.

2.2 Theoretical Formulation

Biomechanical Principles. The circumferential deformation of the duct may be described by the mid-wall circumferential Green strain, which is defined as follows:

$$E_{\theta\theta} = \frac{1}{2}\left[\lambda_{\theta\theta}^2 - 1\right] \tag{1a}$$

where $\lambda_{\theta\theta}$ is the mid-wall stretch ratio ($\lambda_{\theta\theta}$ = c/C); c refers to the mid-wall circumference of the vessel in the loaded state and C refers to the corresponding mid-wall circumference in the zero-stress state (Fung, 1993). Similarly, the axial Green strain is given by

$$E_{zz} = \frac{1}{2}\left[\lambda_{zz}^2 - 1\right] \tag{1b}$$

where λ_{zz} is the local axial stretch ratio defined as the length change in the axial direction from the loaded to the zero-stress state.

The mid-wall circumference in the loaded state was computed from the average of inner and outer radius. The inner radius, r_i, of the vessel duct was computed from the incompressibility condition for a cylindrical vessel as:

$$r_i = \sqrt{r_o^2 - \frac{A_0}{\pi\lambda_z}} \tag{2}$$

where r_o and A_0 are outer radii at the loaded state and the wall area in the no-load state, respectively (Duch, Andersen, Smith, Kassab and Gregersen, 2002). Since all the quantities on the right hand side of Eq. (2) are measured, the loaded inner radius can be computed.

The mean second Piola-Kirchhoff stresses in the circumferential, S_θ, and axial, S_z, directions are given by

$$S_{\theta\theta} = \frac{Pr_i}{h\lambda_{\theta\theta}^2} \tag{3}$$

and

$$S_{zz} = \frac{1}{\lambda_{zz}^2}\left[\frac{Pr_i^2}{h(r_o + r_i)}\right] \tag{4}$$

where P is the pressure and h is the wall thickness determined as the difference between inner and outer radius (Fung, 1993).

2.3 Strain Energy Function

A well known approach to elasticity of bodies capable of finite deformation is to postulate the form of an elastic potential or strain energy function (Green and Adkins, 1960). Following the arguments made by Fung, 1993, we use the following form of strain energy function:

$$\rho_0 W = \frac{C}{2}(\exp[a_1(E_{\theta\theta}^2 - E_{\theta\theta}^{*2}) + a_2(E_{zz}^2 - E_{zz}^{*2}) + 2a_4(E_{\theta\theta}E_{zz} - E_{\theta\theta}^* E_{zz}^*)] - 1) \tag{5}$$

where C, a_1, a_2 and a_4 are constants and starred quantities are strains corresponding to a reference pair of stresses at the homeostatic state (physiological pressure and *in vivo* length). The symbol W represents the strain energy per unit mass of the material; ρ_o is the mass density at zero stres and $\rho_o W$ is the strain energy per unit volume. C has the units of stress (force/area); a_l, a_2 and a_4 are dimensionless constants. The differentiation of the strain energy equation leads to the stress-strain relationship as

$$S_{ij} = \frac{\partial(\rho_o W)}{\partial E_{ij}}, \qquad (i, j = \theta, z) \tag{6}$$

In these formulas, (θ, z) is a set of local right handed cylindrical coordinates with an origin lying on the neutral surface of the duct wall, the axis θ pointing in the circumferential direction and z in the axial direction. S_{ij} is the stress tensor defined in the sense of Kirchhoff, E_{ij} is the strain tensor defined in the sense of Green. The strains are finite and referred to the zero-stress state; $E_{\theta\theta}$, E_{zz}, are normal strains, $E_{\theta z}$=$E_{z\theta}$ are shear strains taken as zero because of the axi-symmetric loading conditions. The subscripts i and j range over 1, 2; with 1 referring to θ; 2 referring to z.

2.4 Determination of Elastic Constants

If we combine Eqns. (5) and (6), we obtain a constitutive relation that relates the circumferential and axial stresses to strains as

$$S_{\theta\theta} = \frac{C}{2}\exp[a_1(E_{\theta\theta}^2 - E_{\theta\theta}^{*2}) + a_2(E_{zz}^2 - E_{zz}^{*2}) + 2a_4(E_{\theta\theta}E_{zz} - E_{\theta\theta}^* E_{zz}^*)](2a_1 E_{\theta\theta} + 2a_4 E_{zz}) \tag{7a}$$

and

$$S_{zz} = \frac{C}{2}\exp[a_1(E_{\theta\theta}^2 - E_{\theta\theta}^{*2}) + a_2(E_{zz}^2 - E_{zz}^{*2}) + 2a_4(E_{\theta\theta}E_{zz} - E_{\theta\theta}^* E_{zz}^*)](2a_2 E_{zz} + 2a_4 E_{\theta\theta}) \tag{7b}$$

The goal of an algorithm to determine the material constants C, a_1, a_2 and a_4 is to minimize the square of the difference between theoretical (proposed function, Eq. (7)) and experimental values of circumferential, $S_{\theta\theta}^e$, and axial, S_{zz}^e, stresses as

$$Error = \sum_{n=1}^{N}\left[(S_{\theta\theta})_n - \left(S_{\theta\theta}^e\right)_n\right]^2 + \left[(S_{zz})_n - \left(S_{zz}^e\right)_n\right]^2 \tag{8}$$

where N represents the total number of experimental points used to determine the material constants of each curve; $S_{\theta\theta}$ and S_{zz} are given by Eqs. (7a) and (7b), respectively. Two approaches were used to minimize the error expressed by Eq. (8) as outlined below.

2.5 Parameter Estimation Methods

The determination of the material constants of the strain energy function was carried out using Mathematica which utilizes the Marquardt-Levenberg (M-L) method for non-linear optimization. The optimized cost function is expressed by Eq. (8). This is a standard method most frequently used for material parameter estimation (Fung, Fronek, and Patitucci, 1979). Alternatively, the genetic algorithm (GA) is a stochastic global search that attempts to mimic biological evolution. GA operates on a population of potential solutions applying the principle of survival of the fittest to produce the best approximation to a solution. At each generation, a new set of approximations is created by the process of selecting individuals according to their level of fitness in the problem domain and breeding them together using operators borrowed from biological genetics. This process leads to the evolution of populations of individuals that are better suited to their environment than the individuals that they were created from, similar to natural selection.The approach is to minimize the cost function in Eq (8) based on a probabilistic rather than numerical approach.

We developed a simple code to implement the GA using the MATLAB Genetic Algorithm Toolbox (The MATLAB Genetic Algorithm Toolbox, 1995). A number of parameters were selected including the size of the population, probability of crossover and mutation; scale for mutation and Tournament probability; and initial guess values for lower and upper limit of C, a_1, a_2 and a_4; and number of generations. The error function (Eq. (8)) was evaluated based on the initial parameters. We set an elitism and recombinant individual as per Tournament algorithm or Roulette Algorithm based on the probability of subsequent tournament algorithm. We selected two parents based on Tournament Algorithm and roulette principle; i.e., the lower the value, the better chance. The selection of children from the two parents was made using cross-over, mutations and elitism. This process was repeated a number of times and the fitness value was computed at each cycle. The converged values represented a minima for Eq. (8).

2.6 Statistical Analysis

The goodness of fit was determined by a correlation coefficient R^2 and root mean square (RMS) error for the relation between calculated (strain energy function) and experimental values. A P-value < 0.05 indicated that the differences between experimental and theoretical values were statistically significant.

3 Results

The material constants C, a_1, a_2 and a_4 were determined using both ML and GA methods. We found no statistically significant differences between any of the parameters determined by the two methods ($P > 0.254$). Hence, we only report the parameters obtained from the more global, GA method.

The material constants for the sham group and CBD obstruction groups for 3 hours, 12 hours, 2 days, 8 days and 32 days are summarized in Table 1. The material constants C, a_1, a_2 and a_4 are shown in the first four columns for the sham group and for each of the experimental groups. Also listed are the homeostatic strains at physiological loading for the circumferential and axial direction ($E^*_{\theta\theta}$ and E^*_{zz}, respectively). Finally, the R^2 that express the goodness of the fit are shown for the circumferential and axial directions, respectively. The RMS error is also computed for each fit as shown in the last two columns of Table 1.

A comparison between the experimental and theoretical values of circumferential and axial stresses is shown in Figures 1(A) and 1(B), respectively. The theoretical values of stresses are those determined from Eq. (7) and the material constants. The data shown are pooled from all groups, sham and experimental. The correlation coefficient for the circumferential (Figure 1(A)) and axial (Figure 1(B)) stresses are 0.946 and 0.952, respectively.

Figure 2(A) shows the time course of change of the product of C and a_1 which reflects the nonlinear rate of change in the circumferential stress. Similarly the rate of change in the axial direction can be quantified by the product of C and a_2 as shown in Figure 2(B). The changes in the circumferential and axial directions are statistically significant ($p < 0.001$).

4 Discussion

4.1 Parameter Estimation

Determination of constitutive equations is an inverse problem. We assume a form of the constitutive relation and based on experimental data of stress and strain, we determine the material properties that give satisfactory agreement between the theorized form and the experi-

Table 1 :

Strain energy constants derived from fitting stress-strain data using genetic algorithms. The values of C, a_1, a_2, and a_4 are given as mean±SEM. The RMS error values are computed from the root mean square of the difference between theoretical and experimental stresses and are expressed as a percentage of the mean experimental stress.

Time (days)	**C (kPa)**	$\mathbf{a_1}$	$\mathbf{a_2}$	$\mathbf{a_4}$	$\mathbf{E_{\theta\theta}}$*	$\mathbf{E_{zz}}$*	$\mathbf{R^2}$ of $\mathbf{S_{\theta\theta}}$	$\mathbf{R^2}$ of $\mathbf{S_{zz}}$	**RMS of $S_{\theta\theta}$ (%)**	**RMS of S_{zz} (%)**
0	2.1 ± 0.31	3.3 ± 0.54	1.9 ± 0.32	1.9 ± 0.44	0.87	0.25	0.955	0.962	17.7	15.8
0.125	4.4 ± 0.48	1.8 ± 0.14	12.7 ± 1.3	1.7 ± 0.37	1.4	0.18	0.937	0.944	18.6	18.0
0.5	10.3 ± 1.1	1.1 ± 0.15	3.1 ± 0.48	0.86 ± 0.1	1.6	0.34	0.965	0.970	15.0	12.6
2	4.5 ± 0.22	1.1 ± 0.07	6.4 ± 0.51	0.52 ± 0.09	1.7	0.26	0.921	0.929	19.6	18.5
8	8.4 ± 0.83	3.7 ± 0.29	3.6 ± 0.69	3.5 ± 0.29	0.98	0.30	0.955	0.957	18.2	14.0
32	5.5 ± 0.44	6.7 ± 0.57	5.7 ± 0.92	4.7 ± 0.76	0.60	0.23	0.826	0.799	29.3	30.1

mental data. It should be noted, however, that there are inherent difficulties with non-linear least squares procedures in that large differences in the values of the material constants may result in very small differences in the data. This is a well known fact about class of nonlinear "inverse" problems (Lanczos, 1965). The difficulty is that the error function given by eq. (8) has many relative minima. In anticipation of this problem, we used two different parameter estimation methods as described below.

4.2 Comparison of M-L and GA Methods

There are several significant differences between the traditional non-linear least squares method (e.g., M-L) and the GA that deserve mention. These differences include 1) GA searches a population of points in parallel, not a single point, 2) GA does not require derivative information or other auxiliary knowledge; only the objective function and the corresponding fitness levels influence the directions of search, 3) GA uses probabilistic transition rules, not deterministic ones, 4) GA works on an encoding of the parameter set rather than the parameter set itself (except where real-valued individuals are used), and 5) traditional methods may miss a local minimum depending on the optimization method employed. In the present study, we did not find any statistically significant differences between the two methods of parameter estimation. Hence, we gained confidence that the parameters estimated minimize the error between the proposed theoretical function and experimental data.

4.3 Limitations of Proposed Model

There are two approaches for the description of the biomechanics of cylindrical wall. In one approach, the duct wall is regarded as a 3-D incompressible material. A second approach relies on the axi-symmetric, thin-walled assumptions and regards the wall as a 2-D compressible membrane structure. The latter approach yields the mean stresses over the wall thickness in the circumferential and axial direction. Such a 2-D approach cannot describe the behavior of a thick-walled cylindrical tube under, for instance, inflation and torsion. The proposed form is limited to a membrane description that involves the mean quantities of stresses and strains.

4.4 A 2-D Constitutive Model of CBD

The present study quantifies the mechanical remodeling process post obstruction due to pressure-overload. A 2-D constitutive model of the CBD describing the circumferential and axial stresses and their respective strains is presented for the normal pig and post obstruction. Although the material constants are phenomenological and do not have a micro-structural basis, they can be interpreted mechanically. The coefficient C dictates the stress scale, the product $C \cdot a_1$ dictates the nonlinear rate of change in the circumferential stress with respect to strain, the product $C \cdot a_2$ has the same meaning in the axial direction, and a_4 indicates the interaction between terms in both circumferential and axial directions (Fung, Fronek, and Patitucci, 1979).

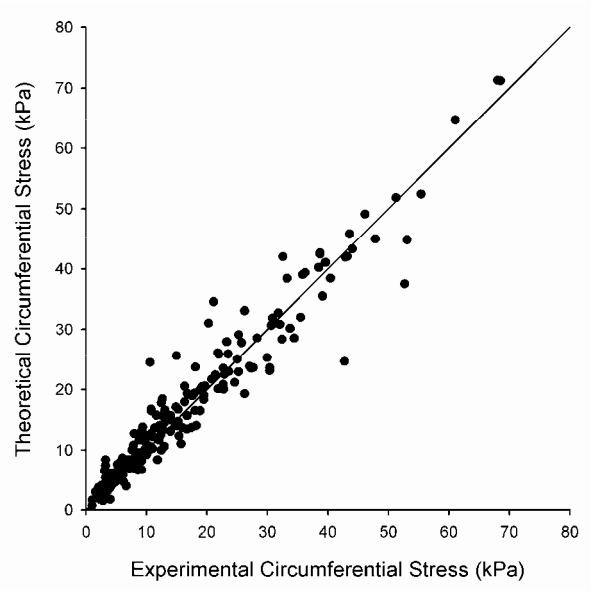

(a)

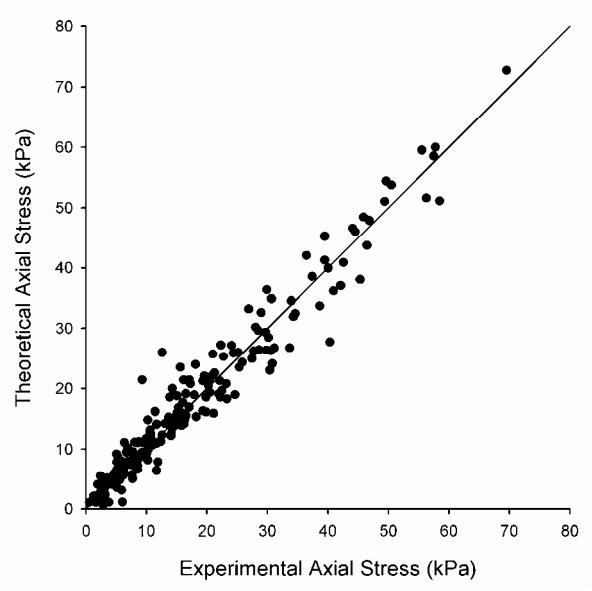

(b)

Figure 1 : A comparison of the theoretical and experimental **A**) circumferential stresses and **B**) axial stresses. The solid line corresponds to the identity relation.

As in most other soft tissues (Fung 1993), exponential mechanical behavior has been observed in the normal (non-obstructed) bile duct *in vitro* (Duch, Petersen, and Gregersen, 1998). The exponential behavior is expedient for organs with reservoir function since low wall stiffness at physiological pressures facilitate wall stretch to accommodate the gall. The steep increase in wall stiffness with higher loads provides a mechanism to avoid overstretch and damage to the tissue. This is in agreement with a previous study of compliance in the intact bile duct where high compliance was found at low pressures and low compliance at high pressures (Slater, Tartter, Delman, Aufses, Dreiling, and Rudick, 1983).

The CBD shows an anisotropic behavior with a much larger capacity to stretch in the longitudinal direction as compared to the circumferential direction during the acute phase as can be seen by the significantly higher value of a_2 at 3 and 12 hours as compared to a_1 (p = 0.045). The fact that the bile duct more readily elongates axially than increases its diameter may 1) mechanically affect the sphincter of Oddi, facilitating leakage of bile at high biliary tract pressures and 2) may contribute to increased stiffness in the circumferential direction [Pandit, Lu and Kassab(2005)].

4.5 Growth and Remodeling of CBD

Obstruction of the CBD leads to an accumulation of bile and hence an increase in the pressure of the biliary duct. The normal pressure range in the bile duct is between 0.6 and 1.3 kPa (Ogawa and Tanaka 1992). With bile duct obstruction the pressure stabilizes at about 3 kPa (Grace, Poston, and Williamson, 1990) because the bile production stops at this pressure. The increase in pressure has both acute and chronic consquences. In relation to the 32-days duration of the experiment, the first 12 hours can be considered as the acute phase. We observed a small increase in $C \cdot a_1$ ("stiffening") acutely (0 to 12 hours) as the duct is distended by the increase in pressure. Subsequently, the stiffness decreased after 2 days. Any surgical procedures that include suturing and anastomosis relating to the repair of obstruction must be mindful of the early chronic changes that make the CBD softer.

Growth and remodeling are clearly observed in this model beyond the acute phase. By day 2, $C \cdot a_1$ is decreased implying "softening" followed by chronic stiffening that reflects the growth and remodeling of the material properties. Axially, the acute response is more apparent here as the duct stiffens axially ($C \cdot a_2$ increases) followed by a more gradual increase in the stiffness during the course of remodeling. The increase in stiffness may be related to the remodeling of the connective tissue.

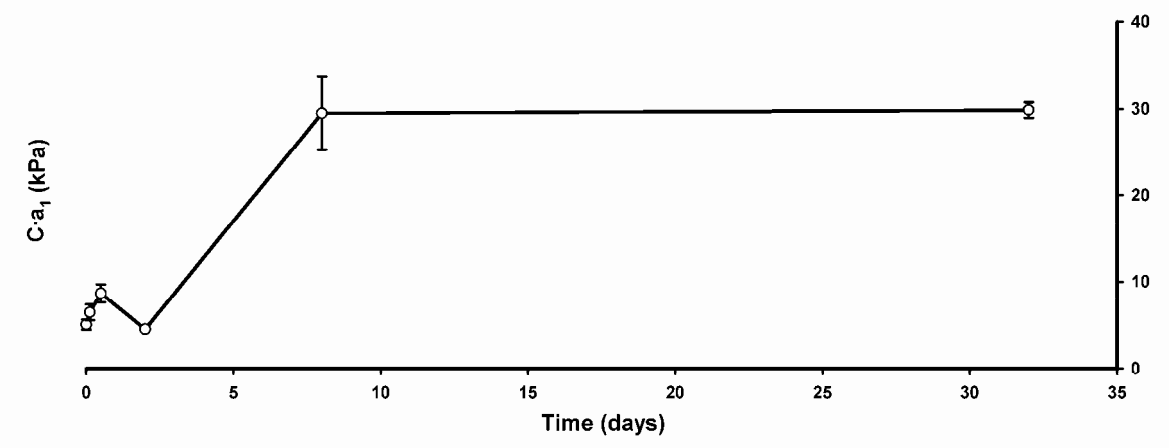

(a)

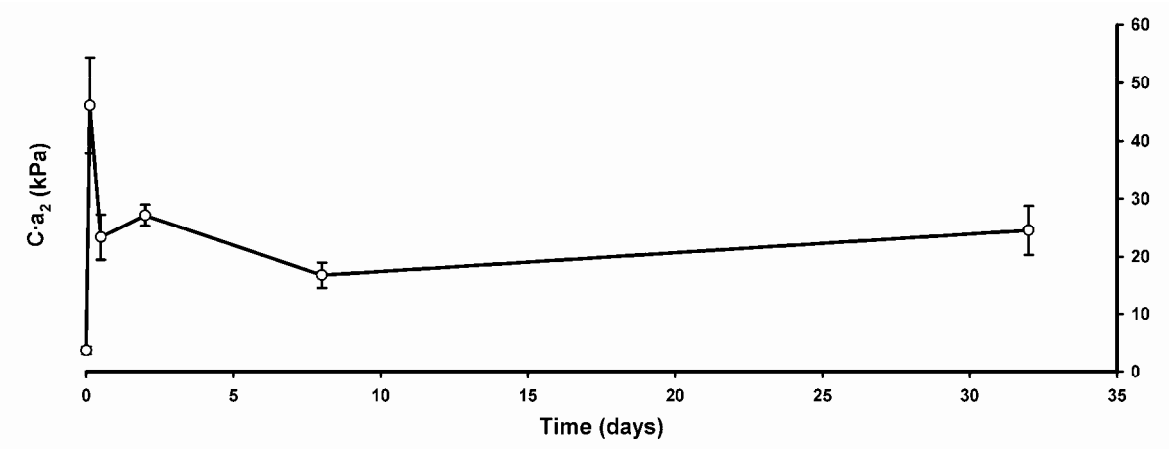

(b)

Figure 2 : The time course of change of the product of material constants **A**) C and a_1 which reflect the non-linear change of stress in the circumferential direction and **B**) C and a_2 which reflect the non-linear change of stress in the axial direction.

It has been previously reported that the connective tissue is more fibrous and contains fewer cells after obstruction as compared to normal ducts (Burdiles, Csendes, Diaz, et al, 1999; Lygidakis, 1984). Post obstruction, the wall consists mostly of fibers in a network grid that rearranges during dilatation by changing the angles it forms with the long axis of the organ (Steiner, Henning and Lierse, 1989).

4.6 Significance of Study

Knowing the material properties of the biliary tract is imperative for understanding normal and abnormal biliary tract function. In this study, we quantified the remodeling of the CBD in terms of the changes in the material properties of the tissue. Such information is clinically important in relation to deciding when a patient should be operated on. Our results show that the tissue is softer early on (acute phase) and may be susceptible to rupture during the surgical treatment. Such information is

equally important for the decision relating to the method of treatment. Simple gall stones may be removed endoscopically and do not constitute a major clinical problem, despite the high incidence in the population. However, intramural cancer or compression of the biliary tract from nearby anatomical structures require surgery or laparoscopy with reconstruction of the biliary tract. The reconstruction has the purpose of reestablishing bile flow from the liver to the intestine and to create stress-free anastomosis. In this process it is important to take into consideration the stresses and strains in circumferential and axial directions in order to obtain the best surgical results with the fewest complications.

Acknowledgement: This research was supported in part by the National Institute of Health-National Heart, Lung, and Blood Institute Grant 2 R01 HL055554-06. We also think the Karen Elise Jensens Foundation, the Danish Research Councils and the Institute of Experimental Clinical Research, Aarhus University.

5 References

Abe, H.; Hayashi, K.; Sato, M. (eds.). (1996): *Data Book on Mechanical Properties of Living Cells, Tissues and Organs*. Tokyo: Springer.

Burdiles, P; Csendes, A; Diaz, J.C., et al (1989). Histological analysis of liver parenchyma and choledocal wall, and external diameter and intraluminal pressure of the common bile duct in controls and patients with common bile duct stones with and without acute suppurative cholangitis. *Hepatogastroenterology*, Vol. 36, 143-6.

Dang, Q.; Duch, B.; Gregersen, H.; Kassab, G.S. (2004): Indicial Response of Growth and Remodeling of Common Bile Duct Post Obstruction. *Am J Physiol Gastrointest Liver Physiol,* vol. 286 no. 3, pp. G420-7.

Duch, B.U.; Petersen, J.A.; Gregersen, H. (1998): Luminal cross-sectional area and tension-strain relation of the porcine bile duct. *Neurogastroenterol Motil*, vol. 10, pp. 203-9.

Duch, B.U.; Andersen, H.L.; Smith, J.; Kassab, G.S.; Gregersen, H. (2002): Structural and mechanical remodeling of the common bile duct during experimental obstruction. *Neurogastro enterol and Motility*, vol. 14, pp. 111-122.

Frierson, H.F. Jr. (1989): The gross anatomy and histology of the gallbladder, extrahepatic bile ducts, Vaterian system, and minor papilla. *Am J Surg Pathol*, vol. 13, pp. 146-62.

Fung, Y.C. (1979): Inversion of a class of nonlinear stress-strain relationships of biological soft tissues. *J Biomech Eng*, vol. 101, pp. 23-27.

Fung, Y.C.; Fronek, K.; Patitucci, P. (1979): Pseudoelasticity of arteries and the choice of its mathematical expression. *Am J Physiol*, vol. 237, pp. H620-H631.

Fung, Y.C. (1993): *Biomechanics: Mechanical Properties of Living Tissues*. 2^{nd} edition, New York: Springer Verlag.

Grace, P.A.; Poston, G.J.; Williamson, R.C. (1990): Biliary motility. *Gut*, vol. 31, pp. 571-82.

Green, A.E.; Adkins, J.E. (1960): *Large deformations and nonlinear continuum mechanics*. Oxford: Oxford University Press.

Gregersen, H.; Kassab, G.S. (1996): Biomechanics of the gastrointestinal tract. *Neurogastroenterology and Motility*, vol. 8, pp. 277-297.

Gregersen, H.; Kassab, G.S.; Fung, Y.C. (2000): The zero-stress state of the gastrointestinal tract. Biomechanical and functional implications. *Digestive Diseases and Sciences*, vol. 45, pp. 2271-2281.

Hasberry, S; Pearcy, MJ (1986). Temperature dependence of the tensile properties of interspinous ligaments of sheep. *J Biomed Eng*; vol. 8, pp. 62-66.

Hauge CW, Mark JB. (1965): Common bile duct motility and sphincter mechanism. I. Pressure measurements with multiple-lumen catheter in dogs. *Ann Surg*, vol. 162, pp. 1028-38.

Hayashi, K. (1993): Experimental approaches on measuring the mechanical properties and constitutive laws of arterial walls. *J Biomech Eng,* vol. 115, pp. 481-8.

Lanczos, C. (1956): *Applied analysis*. Englewood Cliffs, NJ: Prentice-Hall, Inc., 1956.

Lygidakis, NJ (1984). Incidence and significance of ultrastructural changes in the common bile duct in lithiasis with dilatation of the duct. *Acta Chir Scand*, Vol. 150, 665-8.

Ogawa, Y.; Tanaka, M. (1992): Biliary pressure variation in coordination with migrating motor complex of duodenum in patients with cholecystectomy and effects of morphine and cerulean. *Digestive Diseases and Sciences*, vol. 37, pp. 1531-6.

Pandit, A; Lu, X Kassab, G.S (2005). The Biaxial Elastic Material Properties of Porcine Coronary Media and Adventitia. *Am. J. Physiol Hear Circ. Physiol.*, Vol. 288, H2581-2587.

Patel, D.J.; Janicki, J.S.; Vaishnav, R.N.; Young, J.T. (1973): Dynamic anisotropic viscoelastic properties of the aorta in living dogs. *Circ Res,* vol. 32, pp. 93-107.

Roslyn, J.J.; DenBesten, L. (1990): Gallstones and cholecyctitis. In: Moody F. (ed) *Surgical Treatment of Digestive Disease*. Year Book Medical Publishers Inc., Chicago.

Slater, G.; Tartter, P.; Delman, D.; Aufses, A.H. Jr.; Dreiling, D.A.; Rudick J. (1983): Compliance of the extramural portion of the canine common bile duct. *Proc Soc Exp Biol Med*, vol. 173, pp. 344-8.

Steiner, D; Henning, R; Lierse, W (1989). Bioconstruction of the extrahepatic duct system in minipigs. Comparing normal condition with experimental obstruction. *Acta Ana Basel*, vol 136, pp. 159-64.

The MATLAB Genetic Algorithm Toolbox. *IEEE Colloqium on Applied Control Techniques Using MATLAB*, Digest No. 1995/014, 1995.